International Letters of Chemistry, Physics and Astronomy *Online: 2015-09-30*
ISSN: 2299-3843, Vol. 60, pp 129-141
doi:10.18052/www.scipress.com/ILCPA.60.129

Synthesis of N′-(5-arylazosalicylidene)nicotinohydrazide – characterization and DFT analysis

N. Santhi, K.R. Sankaran*

Department of Chemistry, Annamalai University, Annamalainagar, Tamil Nadu, India

E-mail: professorkrs60@gmail.com

Keywords: Nicotinohydrazide, DFT, HOMO-LUMO, MEP.

ABSTRACT. Novel organic compounds N′-(5-arylazosalicylidene)nicotinohydrazide (**3**) and their derivatives **(4** and **5)** were synthesized and their structures were elucidated and confirmed by the spectral techniques like IR, ^{1}H, ^{13}C and 2D NMR. The stable configuration of the above structures achieved theoretically using DFT method with the 6-31G(d,p) chosen level of basis set. Molecular orbital properties like HOMO, LUMO, MEP were analyzed and reported. The topological properties behavior of atoms in molecules were studied using AIM and NBO analysis which reveals the presence of bonding, ring formation and hydrogen bonding in the compounds. Finally the electrical properties like dipolemoment, polarizability, hyperpolarizability have been studied using DFT at the same level of basis set and provides information about material science applications of the above synthesized compounds.

1. INTRODUCTION

Hydrazide derivatives have been of great interest because of their role in natural and synthetic organic chemistry. Many products which contain a hydrazide subunit exhibit biological activity such as molluscicides, anthemintic, hypnotic, insecticidal, activity and fluorescent brightness [1]. Many hydrazine compounds showed good anticancer bioactivities. hydrazone functional group increases the lipophilicity of parent amine and amides and results in the enhancement of absorption through biomembranes and enables them to cross bacterial and fungal membranes [2-4].

Hydrazone functional group increases the lipophilicity of parent amides and results in the enhancement of absorption through biomembranes and enables them to cross bacterial and fungal membranes [5, 6]. Their metal compounds have found applications in various chemical processes like non-liner optics, sensors, medicine etc [7].

Schiff bases hydrazones are widely used in analytical chemistry as selective metal extracting agents as well as in spectroscopic determination of certain transition metals [8,9]. Schiff bases complexes have been widely studied because they have industrial, fungicide, antibacterial, anticancer and herbicidal applications [10, 11]. Schiff base play a vital role in inorganic chemistry as they easily form stable complexes. Schiff bases derived from condensation of nicotinic acid hydrazide with aldehydes represent an important compounds of great interest due to their importance in biological, pharmacological and clinical applications. The hydrazine derivatives are used as fungicides and in the treatment of some diseases such as tuberculosis leprosy and mental disorders [12-14].

2. EXPERIMENTAL

Nicotinohydrazides was purchased from sigma Aldrich. All other chemicals were used as analytic grade. Reaction was monitored by TLC. The melting point is measured on open capillaries and are in corrected.

2.1. Synthesis of N′-(5- arylazosalicylidene)nicotinohydrazide and its derivatives

N′-(5-arylazosalicylidene)nicotinohydrazide **3** and its derivatives were prepared according to the literature [15]. To solution of N′-5-arylazosalicylaldehyde **1** (0.38 g, 1.5 mmol) and nicotinohydrazide **2** (0.21 g, 1.5 mmol) in methanol five drops of glacial acetic acid were added and the reaction mixture was refluxed for 6 h and then the mixture was poured into ice cold water. The mixture was kept overnight at room temperature. It was filtered, washed and recrystallized from methanol. The physical data shown in Table 1.

2.2. Spectral Measurements

The FT-IR spectrum is recorded in the range 4000–400 cm^{-1} with a resolution of ± 4 cm^{-1} and an accuracy of ±0.01 cm^{-1} on Nicolet Avatar 360 FT-IR spectrometer. The sample was mixed with KBr and the pellet technique was adopted. The proton spectrum at 400 MHz and proton decoupled ^{13}C NMR spectrum at 100 MHz in DMSO-d_6 were recorded at room temperature on Bruker 400 MHz spectrometer using 10 mm sample tube, samples were prepared by dissolving about 10 mg of the sample in 0.5 mL of DMSO-d_6 containing a few drops at TMS for ^{13}C.

2.3. Computational Studies

Geometry optimization was carried out according to density functional theory available in Gaussian-03 package using B3LYP/6-31G(d,p) basis set [16].

3. RESULTS AND DISCUSSION

The N′-(5-arylazosalicylidene)nicotinohydrazide **3** and its derivatives (**4** and **5**) were obtained by refluxing 5-arylazosalicylaldehyde **1** with nicotinohydrazide **2** and **5** drops of acetic acid in methanol (**Scheme 1**). All the synthesized compounds are characterized by the FT-IR and the high-resolution ^{1}H and ^{13}C NMR spectra and analyzed. We discussed in detail the compound **3** only.

The prominent peaks in the range 3430–3190, 1650–1800 and 1640–1560 cm^{-1} [14] in the IR spectrum are attributed to ν_{N-H} and ν_{O-H}, $\nu_{C=O}$ and $\nu_{C=N}$ and $\nu_{C=C}$ modes respectively. The observation of lower $\nu_{C=O}$ is due to the extended conjugation of C=O group with the nearby pyridine ring. The bending vibration of the O–H group appeared around 1350 cm^{-1} in all the hydrazides. The sharp peak around 3020 cm^{-1} in the IR spectrum of **3** due to the aromatic ν_{C-H} mode. In hydrazide strong peak for N=N group is observed at 1480 cm^{-1} [17]. Aromatic C–H out-of-plane bending vibration appeared around 840 and 700 cm^{-1} [18]. The experimental and calculated (DFT) IR spectral data of **3-5** is displayed in **Table 1.**

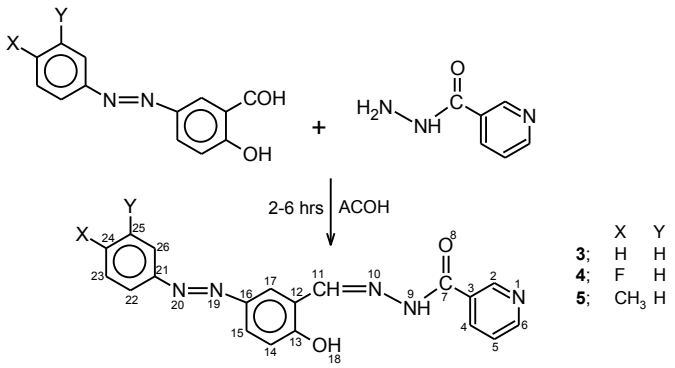

Scheme 1

Table 1. Physical, experimental and computational IR data (cm^{-1}) of synthesized nicotinohydrazides (3-5)

Compounds	Physical data		
	Colour	Yield (%)	m.p. (°C)
3	Orange	88	>230
4	Orange	80	208-210
5	Orange	85	197-199

IR data					
3		**4**		**5**	
Exp.	**DFT**	**Exp.**	**DFT**	**Exp.**	**DFT**
3422	3404	3391	3404	3392	3404
3219	3247	3211	3244	3210	3247
3027	3030	3040	3030	3028	3031
1709	1716	2918	2945	2920	2922
1607	1601	1795	1716	1748	1716
1466	1485	1606	1626	1633	1626
1420	1420	1489	1491	1486	1503
1378	1382	1416	1402	1417	1421
1317	1285	1353	1382	1351	1332
1191	1195	1306	1285	1305	1284
1163	1148	1226	1231	1195	1197
1117	1096	1028	999	1168	1148
1089	1092	971	951	1084	1092
1028	999	893	895	1026	999
897	894	838	824	972	972
829	826	782	800	892	895
769	760	702	697	825	828
694	697	469	461`	781	757
506	482	–	–	702	697
465	461	–	–	511	534
–	–	–	–	458	459

3.1. Spectral (^{1}H and ^{13}C NMR) calculation

The ^{1}H and ^{13}C NMR chemical shifts were determined theoretically by DFT method in DMSO-d_6 using the basis set B3LYP/6-311+G(2d,p) GIAO and the salvation model PCM (SCRF=PCM) [19]. The scale factors are based on the reference compounds used as well as on the basis set employed for DFT calculation. Experimental and computational ^{1}H and ^{13}C NMR spectral data of hydrazide **3-5** are listed in **Table 2.**

Table 2. Experimental and computational ^{1}H and ^{13}C NMR spectral data (ppm) of 3-5

Protons	73		74		75	
	Obs.	DFT	Obs.	DFT	Obs.	DFT
H-2	9.12	9.33	9.12	9.31	9.12	9.30
H-4	8.31	8.82	8.31	8.82	8.31	8.82
H-5	7.61	7.87	7.61	7.90	7.61	7.90
H-6	8.78	9.15	8.78	9.14	8.79	9.14
H-11	8.78	8.60	8.78	8.56	8.79	8.57
H-14	7.13	7.55	7.13	7.53	7.14	7.52
H-15	7.95	8.48	7.95	8.47	7.90	8.47
H-17	8.32	8.55	8.30	8.49	8.26	8.51
H-22	7.95	8.51	7.95	8.54	7.80	8.43
H-23	7.42	7.88	7.42	7.54	7.39	7.72
H-24	7.42	7.90	–	–	–	–
H-25	7.42	8.06	7.42	7.68	7.39	7.80
H-26	7.95	8.44	7.95	8.40	7.80	8.20
CH_3	–	–	–	–	2.51	2.56
Carbons						
C-2	148.62	153.65	148.63	153.54	148.60	153.51
C-3	128.80	135.11	129.10	135.02	129.89	135.07
C-4	135.52	144.00	135.49	144.02	135.50	144.02
C-5	123.75	129.55	124.42	129.50	123.75	129.48
C-6	152.44	160.71	152.47	160.56	152.46	160.52
C-7	163.23	167.55	162.14	167.62	161.64	167.60
C-11	152.64	153.89	146.49	153.81	146.68	153.98
C-12	119.59	124.34	119.76	124.09	119.68	124.01
C-13	162.15	171.33	160.38	171.29	159.95	170.91
C-14	117.80	121.62	117.34	121.64	117.25	121.52
C-15	125.89	143.82	126.11	143.89	125.98	143.53
C-16	143.56	152.20	144.87	152.26	145.06	152.41
C-17	122.68	121.76	122.94	121.69	122.81	121.53
C-21	152.64	159.53	152.62	156.46	150.03	157.54
C-22	122.10	117.99	124.51	120.86	122.26	117.92
C-23	129.13	134.36	116.42	121.68	129.89	135.66
C-24	139.82	137.72	152.62	174.78	141.02	151.91
C-25	129.13	134.60	116.42	120.74	129.89	134.86

3.1.1. Analysis of ^{1}H NMR spectra of nicotinohydrazides 3-5

The 400 MHz NMR spectrum of N′-(5-phenylazosalicylidene)- nicotinohydrazide **3** reveals high intense singlets at 9.12 and 8.78 ppm for *ortho* protons with respect to nitrogen *i.e.,* H(2) and H(6) of the nicotinoyl ring respectively. A doublet observed at 8.31 ppm and a signal observed at 7.61 ppm are assigned to the ring protons H(4) and H(5) respectively of nicotinoyl ring.

Among the remaining signals, the high frequency signal centered at 8.79 ppm is assigned to the azomethine proton H(11). The low frequency doublet observed at 7.13 ppm (J = 6.00 Hz) is assigned to the *ortho* proton with respect to OH group *i.e.,* H(14). The ^{1}H NMR spectrum further reveals a signal at 7.42 ppm (integral corresponds to three protons) and a broad signal at 7.95 ppm

(integral corresponds to two protons) for the *meta* and *para* protons of the phenyl ring *i.e.,* H(23), H(24) and H(25) and *ortho* protons of the phenyl ring [H(22) and H(26)] respectively. For H(17), a signal at 8.32 ppm was observed. The remaining signal at 7.95 ppm is assigned to the proton H(15). In a similar manner assignments are done for other hydrazides **4** and **5**.

3.1.2. Analysis of ^{13}C NMR spectra of nicotinohydrazides 5-7

^{13}C NMR spectra at 100 MHz have been recorded in DMSO-d_6 for **3**. The *ipso* carbons can be easily distinguished from other aromatic carbons based on small intensities.

The high frequency signal at 163.23 ppm is due to the carbonyl carbon [C(7)] of the hydrazide moiety. The hydroxy bearing carbon C(13) resonates at 162.15 ppm. For the *ipso* carbons C(3), C(12), C(16) and C(21) signals were observed at 128.80, 119.59, 143.56 and 152.64 ppm. Among these signals, the low frequency signal at 119.59 ppm is assigned to the quaternary carbon C(12) since it is *ortho* with respect to electron releasing OH group. Among the remaining signals at 128.80, 143.56 and 152.64 ppm, the signal at 143.56 ppm is assigned to the *ipso* carbon C(16) which is attached to the nitrogen atom N(19) and also *para* with respect to OH group. The signal at 152.64 ppm is due to C(21) which is attached to nitrogen atom N(20). Obviously, the remaining signal at 128.80 ppm is due to C(3). The low frequency signal at 117.80 ppm is assigned to C(14) carbon and this assignment is based on the known shielding magnitude of OH group. The C(15) and C(17) carbons resonate at 125.89 and 122.68 ppm respectively.

From the intensities, the signals at 122.10 and 129.13 ppm are assigned to *ortho* [C(22) and C(26)] and *meta* [C(23) and C(25)] carbons and the signal at 139.82 ppm is assigned to *para* carbon [C(24)]. The signals at 152.44 and 148.62 ppm are assigned to the *ortho* carbons *i.e.,* C(6) and C(2) respectively with respect to nitrogen of the pyridine ring. The remaining signals at 135.52 and 123.75 ppm are assigned to the ring carbons C(4) and C(5) of the pyridine ring and this assignment is based on the comparison of these signals with those of nicotinoylhydrazine. The azomethine carbon C(11) resonates at 152.64 ppm. In a similar manner assignments are done for the other nicotinohydrazides **4** and **5**.

3.2. Geometric parameters

From the optimized structures, geometrical parameters were derived (**Table 3**). The calculated bond lengths of C3–C7 and C11–C12 are in agreement with the bond lengths expected for a single bond. The observed torsional angles indicate all the atoms lie in the same plane except the pyridine ring. The torsional angles C4–C3–C7–N9[≈158°] and C2–C3–C7–N9[≈24°] indicate the distortion of pyridine ring from other moieties. Further, the torsional angles C2–C3–C7–O8[≈156°] and C4–C3–C7–O8[≈21°] also support the distorted nature of pyridine ring from other moieties lying in the same plane.

Table 3. Selected geometric parameters [bond lengths (Å), bond angles (°) and torsional angles (°)] in nicotinohydrazides 3-5

Geometric parameters	3	4	5
Bond length			
C3–C7	1.50	1.50	1.50
C7–O8	1.22	1.22	1.22
C7–N9	1.39	1.39	1.39
N9-N10	1.36	1.36	1.36
N10-C11	1.29	1.29	1.29
C11-C12	1.45	1.45	1.45
C13-O18	1.34	1.34	1.34
C16-N19	1.41	1.41	1.41
N19-N20	1.26	1.26	1.26
N20-C21	1.42	1.42	1.42
O18-H18	0.99	0.99	0.99

C24-F27/C24-C27		1.35	1.51
C23-C27/C23-N27		-	-
Bond angle			
C3-C7-O8	122.6	122.6	122.6
C3-C7-N9	114.8	114.8	114.8
O8-C7-N9	122.6	122.5	122.6
C7-N9-N10	119.5	119.4	119.5
N9-N10-C11	119.2	119.3	119.2
N10-C11-C12	120.9	120.9	121.0
H18-O18-C13	109.4	109.4	109.4
C16-N19-N20	115.0	115.1	115.0
N19-N20-C21	114.8	114.7	114.8
Torsional angle			
C4-C3-C7-N9	-158.3	-158.2	--158.1
C4-C3-C7-O8	21.2	21.3	21.4
C2-C3-C7-O8	-156.6	–156.5	–156.4
C2-C3-C7-N9	23.9	24.0	24.1
C3-C7-N9-N10	-179.4	--179.4	-179.4
O8-C7-N9-N10	1.1	1.1	1.1
C7-N9-N10-C11	-175.0	--174.9	-174.8
N9-N10-C11-C12	-179.8	–179.8	-179.8
N10-C11-C12-C13	-0.5	--0.5	-0.5
N10-C11-C12-C17	179.6	179.6	179.6
C11-C12-C13-O18	-0.0	--0.1	–0.0
C12-C13-O18-H18	-0.0	--0.1	-0.1
C17-C16-N19-N20	0.2	0.3	0.3
C15-C16-N19-N20	-179.8	--179.7	-179.7
C16-N19-N20-C21	-180.0	--180.0	-180.0
N19-N20-C21-C22	0.2	0.4	0.4
N19-N20-C21-C26	-179.8	--179.6	-179.6

Table 4. NBO analysis of 3-5 by DFT method [B3LYP/6-311G(d,p)]

Donor NBO	Acceptor NBO	3	4	5
BD(2)C3-C2	BD*(2)C7-O8	17.76	17.77	17.69
BD(2)C3-C2	BD*(2)C4-C5	20.95	20.94	20.96
BD(2)C3-C2	BD*(2)N1-C6	16.44	16.42	16.45
BD(2)C4-C5	BD*(2)C3-C2	17.83	17.84	17.83
BD(2)C4-C5	BD*(2)N1-C6	29.29	29.28	29.29
BD(2)N1-C6	BD*(2)C3-C2	27.28	27.30	27.25
BD(2)N1-C6	BD*(2)C4-C5	12.74	12.73	12.74
BD(2)C26-C21	BD*(2)N19-N20	20.10	20.34	20.69
BD(2)C26-C21	BD*(2)C22-C23	19.04	20.76	19.17
BD(2)C26-C21	BD*(2)C25-C24	19.38	19.07	18.32
BD(2)C22-C23	BD*(2)C26-C21	19.36	17.30	18.31
BD(2)C22-C23	BD*(2)C25-C24	20.54	23.03	20.76
BD(2)C25-C24	BD*(2)C26-C21	20.93	21.49	22.35
BD(2)C25-C24	BD*(2)C22-C23	18.51	17.03	17.39
BD(2)N19-N20	BD*(2)C26-C21	10.70	10.71	10.70
BD(2)C14-C15	LP*(1)C13	59.28	59.13	59.16
BD(2)C14-C15	BD*(2)C17-C16	15.54	15.55	15.56
BD(2)C17-C16	LP (1)C12	47.18	47.08	47.23
BD(2)C17-C16	BD*(2)C14-C15	21.28	21.20	21.28
BD(2)C17-C16	BD*(2)N19-N20	16.53	16.77	16.37
BD(2)C11-N10	LP(1)C12	12.92	12.94	12.87
LP(1)N9	BD*(2)C11-N10	27.66	27.78	27.56
LP(1) N9	BD*(2)C7-O8	47.48	47.30	47.45
LP(2)O8	BD*(1)N9-C7	29.17	29.21	29.15

LP(2)O8	BD*(1)C7-C3	19.83	19.82	19.84
LP(1)N1	BD*(1)C3-C2	10.45	10.45	10.44
LP(1)C12	BD*(2)C17-C16	72.92	73.14	72.45
LP(1)C12	BD*(2)C11-N10	72.97	72.70	73.36
LP(1)N10	BD*(1)O18 -H18	22.74	22.84	22.70
LP(2)O18	LP*(1) C13	74.95	75.16	74.58
LP*(1)C13	BD*(2)C14 -C15	–	49.14	–
LP(2)F27	BD*(2)C25-C24	–	20.69	–
LP(2)O18	BD*(2)C13-C14	–	–	–
BD(2)C12-C17	BD*(2)C13-C14	–	–	–
BD(2)C12-C17	BD*(2)C16-C15	–	–	–
BD(2)C12-C17	BD*(2)C11-N10	–	–	–
BD(2)C13-C14	BD*(2)C16-C15	–	–	–
BD(2)C13-C14	BD*(2)C12-C17	–	–	–
BD(2)C16-C15	BD*(2)C12-C17	–	–	–
BD(2)C16-C15	BD*(2)C13-C14	–	–	–
BD(2)C16-C15	BD*(2)N19-N20	–	–	–
BD(2)N19-N20	BD*(2)C16-C15	–	–	–
LP(2)O28	BD*(1)C23-N27	–	–	–
LP(2)O28	BD*(1)N27-O29	–	–	–
LP(3)O28	BD*(2)N27-O29	–	–	–
LP(2)O29	BD*(1)C23- N27	–	–	–
LP(2)O29	BD*(1)N27-O28	–	–	–
BD(2)C21-C22	BD*(2)N19-N20	–	–	–
BD(2)C21-C22	BD*(2)C26-C25	–	–	–
BD(2)C21-C22	BD*(2)C23-C24	–	–	–
BD(2)C26-C25	BD*(2)C21-C22	–	–	–
BD(2)C26-C25	BD*(2)C23-C24	–	–	–
BD(2)C23-C24	BD*(2)C21-C22	–	–	–
BD(2)C23-C24	BD*(2)C26-C25	–	–	–
BD(2)C23-C24	BD*(2)N27-O29	–	–	–
BD(2)N19-N20	BD*(2)C21-C22	–	–	–
BD(2)N27-O29	LP(3)O28	–	–	–
From unit 1 To unit 2		–	–	–
BD(1)C13-018	LP*(1)H18	–	–	–
LP(1) N10	LP*(1)H18	–	–	–
LP(1)O18	LP*(1)H18	–	–	–
LP(3)O18	LP*(1)H18	–	–	–

3.3. Natural bond orbital analysis

NBO analysis at B3LYP/6-31G(d,p) level were carried out for the hydrzides **3-5** and the important second order perturbative estimates of donor-acceptor interactions are displayed in **Table 4**. The interaction between filled and empty NBO's can be described as a hyperconjugative electron transfer process from the donor (filled) to the acceptor (vacant) orbital and the energy lowering due to this interaction is expressed as $\boldsymbol{E_2}$. The delocalization energy corresponding to the transfer of electrons from the bonding orbital of N19–N20 to the antibonding orbital of C26–C21 (≈10.7 kcal mol^{-1}) is lower than that of the energy corresponding to the transfer of electrons from the bonding orbital of C26–C21 to the antibonding orbital of N19–N20 (≈20 kcal mol^{-1}) in hydrazides **3-5**. Further, it is also observed that the delocalization energy corresponding to the transfer of electrons from the bonding orbital of C11–N10 to the p orbital of C12 is lower (≈13 kcal mol^{-1}) relative to the reverse transfer of electrons (≈73 kcal mol^{-1}) in **3-5**. This confirms that electron transfer occurs from phenolic ring to the azomethine side chain in **3-5**.

The lone pair of electrons available on oxygen atom O(18) is delocalized on to the nearby C(13) *p**-orbital and this is the primary delocalization (≈75 kcal/mol) seen in the hydrazides **3-5**. The hyper conjugative interaction energies involving C(12) *p*-orbital with the antibonding orbitals of *vicinal* C(17)–C(16) and C(11)–N(10) bonds are also found to be very high around 73 kcal mol^{-1} in the hydrazides **3-5**. Most stabilizing interactions take place between *vicinal* NBOs. Besides these, some interactions between remote filled and unfilled orbitals are also present. The main stabilized interaction involves the N(10) lone pair as donors and the O(18)–H(18) antibonding orbital [σ*(O(18)–H(18))] as acceptor in hydrazides **3-5** (≈23 kcal $mol^{-1)}$.

3.4. Atoms in molecules (AIM) analysis

Atoms in molecules electron density topological analysis[20] carried out for hydrazide **3** using AIM-All package[21] revealed the existence of 44 bond critical points (BCPs) with (3, –1) topology. **Table 5**.

For shared (covalent) interaction between two atoms charge density at BCP is very high (ρBCP ~10–1 a.u), whereas for closed shell interactions ρBCP is small (~10^{-3} a.u). The high values of ρ_{BCP} observed for all bonds except between non-bonded atoms N10…H18 indicate the interaction between two atoms is covalent in nature. The negative values obtained for the Laplacian of electron density ($\nabla^2\rho_{BCP}$) for N1–C2, N1–C6, C3-C7, C7-O8, C7-N9, N9-N10, N10-C11, C13-O18, C16-N19, N19–N20, C21–N20, N9-H9 and O18-H18 bonds are a clear indication that the electronic charge is locally arranged within the region of inter atoms leading to an interaction named as covalent or polarized bonds and being characterized by large ρ values.

Besides these BCP was also located between the non-bonded H(18) and N(10) atoms in hydrazides **3-5**. Ring critical point of phenyl ring attached to N(20) is slightly having higher electron density compared to the phenolic ring. Another ring critical point was also observed in hydrazides [C(12)–C(13)–O(18)–H(18)–N(10)–C(11)] thus reinforcing the idea of a strong intramolecular hydrogen bond for the hydrazides **3-5**. As pointed by Bader a relationship exists between the hydrogen bond strength and the density in the BCP.

Table 5. Topological properties at BCP (3, –1) in relevant bonds of 3-5

Compds.	Bond (A···B)	ρ_{BCP}	$-\nabla^2\rho_{BCP}$	ε	λ_1	λ_2	λ_3	$\lvert\lambda_1\rvert/\lambda_3$	G	V	H	G_b/ρ_{BCP}
3	N1-C2	0.347	1.0775	0.1277	–0.7564	–0.6708	0.3497	2.1630	0.2955	–0.8604	–0.5649	0.8516
	N1-C6	0.344	1.0428	0.1077	–0.7470	–0.6743	0.3785	1.9736	0.3033	–0.8674	–0.5640	0.8817
	C3-C7	0.266	0.6616	0.1009	–0.5418	–0.4921	0.3723	1.4552	0.0614	–0.2882	–0.2268	0.2308
	C7-O8	0.408	-0.0663	0.1037	–1.0638	–0.9639	2.0940	0.5080	0.7152	–1.4139	–0.6987	1.7529
	C7-N9	0.307	0.9348	0.1171	–0.6689	-0.5988	0.3329	2.0093	0.2316	–0.6969	–0.4653	0.7544
	N9-N10	0.359	0.7064	0.0887	-0.8130	-0.7468	0.8534	0.9527	0.1785	-0.5336	-0.3551	0.4972
	N10-C11	0.367	0.5349	0.2679	-0.8560	-0.6751	0.9962	0.8593	0.4962	-1.1262	-0.6300	1.3520
	C13-O18	0.308	0.3478	0.0081	-0.6619	-0.6566	0.9708	0.6818	0.3982	-0.8834	-0.4851	1.2929
	C16-N19	0.304	0.9814	0.0916	-.0.6559	-0.6009	0.2754	2.3816	0.1529	-0.5512	-0.3983	0.5030
	N19-N20	0.454	1.0408	0.1327	-1.0840	-0.9570	1.0002	1.0839	0.2732	-0.8067	-0.5334	0.6022
	N20-C21	0.301	0.9651	0.0672	-0.6449	-0.6043	0.2841	2.2700	0.1444	-0.5300	-0.3856	0.4797
	N9-H9	0.342	1.8104	0.0581	-1.3176	-1.2452	0.7525	1.7510	0.0538	-0.5603	-0.5064	0.1573
	O18-H18	0.336	1.9599	0.0165	-1.7751	-1.7462	1.5613	1.1369	0.0715	-0.6330	-0.5615	0.2128
	N10…..H18	**0.043**	**-0.1125**	**0.0326**	**-0.0670**	**-0.0649**	**0.2444**	**0.2741**	**0.0302**	**-0.0322**	**-0.0021**	**0.7023**
4	N1-C2	0.347	1.0778	0.1277	–0.7565	–0.6709	0.3496	2.1639	0.2955	–0.8604	–0.5649	0.8516
	N1-C6	0.344	1.0427	0.1076	–0.7469	–0.6744	0.3786	1.9728	0.3034	–0.8674	–0.5640	0.8812
	C3-C7	0.266	0.6621	0.1010	–0.5421	–0.4923	0.3723	1.4561	0.0615	–0.2885	–0.2270	0.2313
	C7-O8	0.408	-0.0672	0.1037	–1.0641	–0.9641	2.0953	0.5079	0.7155	–1.4143	–0.6987	1.7554
	C7-N9	0.307	0.9349	0.1167	–0.6682	-0.5984	0.3318	2.0139	0.2308	–0.6953	–0.4645	0.7518
	N9-N10	0.359	0.7074	0.0888	-0.8138	-0.7474	0.8538	0.9532	0.1787	-0.5342	-0.3555	0.4982
	N10-C11	0.367	0.5337	0.2686	-0.8560	-0.6747	0.9970	0.8586	0.4965	-1.1264	-0.6299	1.3514
	C13-O18	0.308	0.3477	0.0082	-0.6626	-0.6571	0.9720	0.6817	0.3986	-0.8841	-0.4855	1.2946
	C16-N19	0.304	0.9828	0.0927	-.0.6558	-0.6001	0.2731	2.4013	0.1547	-0.5550	-0.4004	0.5084
	N19-N20	0.453	1.0374	0.1337	-1.0821	-0.9545	0.9991	1.0831	0.2727	-0.8049	-0.5321	0.6020
	N20-C21	0.302	0.9708	0.0782	-0.6509	-0.6037	0.2839	2.2927	0.1453	-0.5333	-0.3880	0.4806
	N9-H9	0.342	1.8105	0.0581	-1.3177	-1.2454	0.7526	1.7509	0.0538	-0.5602	-0.5064	0.1574
	O18-H18	0.336	1.9592	0.0165	-1.7747	-1.7459	1.5613	1.1367	0.0715	-0.6328	-0.5613	0.2129
	N10…..H18	**0.043**	**-0.1128**	**0.0324**	**-0.0673**	**-0.0652**	**0.2453**	**0.2744**	**0.0303**	**-0.0324**	**-0.0021**	**0.7014**
	C24-F27	0.255	0.1409	0.0689	-0.4969	-0.4648	1.1026	0.4507	0..3925	-0.7497	-0.3573	1.5362
5	N1-C2	0.347	1.0771	0.1276	–0.7563	–0.6707	0.3498	2.1621	0.2955	–0.8603	–0.5648	0.8528
	N1-C6	0.344	1.0428	0.1079	–0.7470	–0.6742	0.3785	1.9736	0.3034	–0.8674	–0.5640	0.8812
	C3-C7	0.266	0.6615	0.1008	–0.5417	–0.4921	0.3724	1.4546	0.0614	–0.2882	–0.2268	0.2311
	C7-O8	0.407	-0.0657	0.1037	–1.0635	–0.9636	2.0927	0.5082	0.7150	–1.4135	–0.6985	1.7550
	C7-N9	0.307	0.9354	0.1176	–0.6695	-0.5990	0.3331	2.0099	0.2318	–0.6974	–0.4656	0.7553
	N9-N10	0.358	0.7058	0.0884	-0.8125	-0.7465	0.8532	0.9522	0.1784	-0.5333	-0.3549	0.4978

	N10-C11	0.367	0.5359	0.2670	-0.8556	-0.6753	0.9950	0.8599	0.4959	-1.1257	-0.6298	1.3501
	C13-O18	0.307	0.3488	0.0085	-0.6607	-0.6551	0.9670	0.6832	0.3972	-0.8816	-0.4844	1.2921
	C16-N19	0.304	0.9807	0.0910	-.0.6562	-0.6015	0.2771	2.3681	0.1516	-0.5484	-0.3968	0.4984
	N19-N20	0.453	1.0377	0.1330	-1.0820	-0.9551	0.9994	1.0826	0.2726	-0.8047	-0.5321	0.6018
	N20-C21	0.302	0.9717	0.0727	-0.6474	-0.6035	0.2792	2.3188	0.1480	-0.5390	-0.3910	0.4797
	N9-H9	0.342	1.8102	0.0581	-1.3174	-1.2450	0.7522	1.7514	0.0539	-0.5602	-0.5064	0.1577
	O18-H18	0.336	1.9610	0.0166	-1.7759	-1.7469	1.5618	1.1371	0.0716	-0.6334	-0.5618	0.2130
	N10…..H18	**0.043**	**-0.1125**	**0.0328**	**-0.0669**	**-0.0648**	**0.2443**	**0.2738**	**0.0302**	**-0.0322**	**-0.0021**	**0.7023**

Ring		**Ring parameters**		
		$\rho \times 10^2$		
		73	**74**	**75**
1	N1–C6–C5–C4–C3–C2	2.23	2.23	2.23
2	C21-C22-C23-C24-C25-C26	2.01	2.00	2.01
3	C12–C13–C14–C15–C16–C17	1.96	1.95	1.96
4	C12-C13-O18-H18-N10-C11	1.60	1.60	1.60

3.5. MEP surfaces

Three dimensional distribution of MEP (molecular electrostatic potential) is highly useful in predicting the reactive behaviour of the molecule. The molecular electrostatic potential MEP surface is an overlaying of the electrostatic potential on to the isoelectron density surface. This is a valuable tool for describing over all molecule charge distribution as well as anticipating sites of electrophilic addition. The molecular electrostatic potential surface (MEP) has been plotted for hydrazides **5-7** and the diagram is given in **Fig. 1**. Region of negative charge (red colour) is seen around the electronegative oxygens O(8) and O(18) in all the hydrazides.

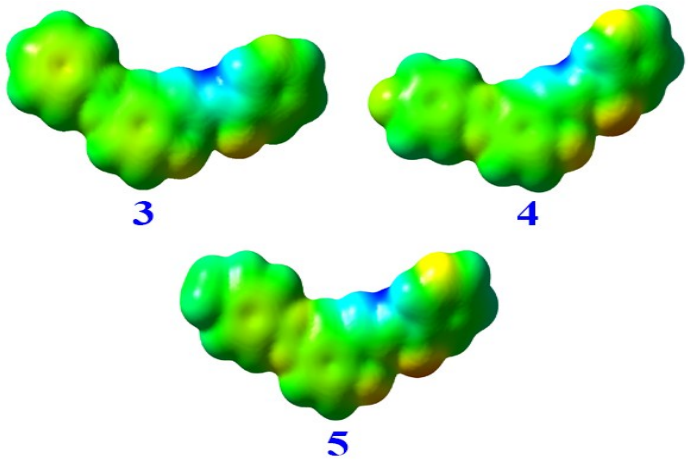

Fig. 1. MEP surface picture of 3-5

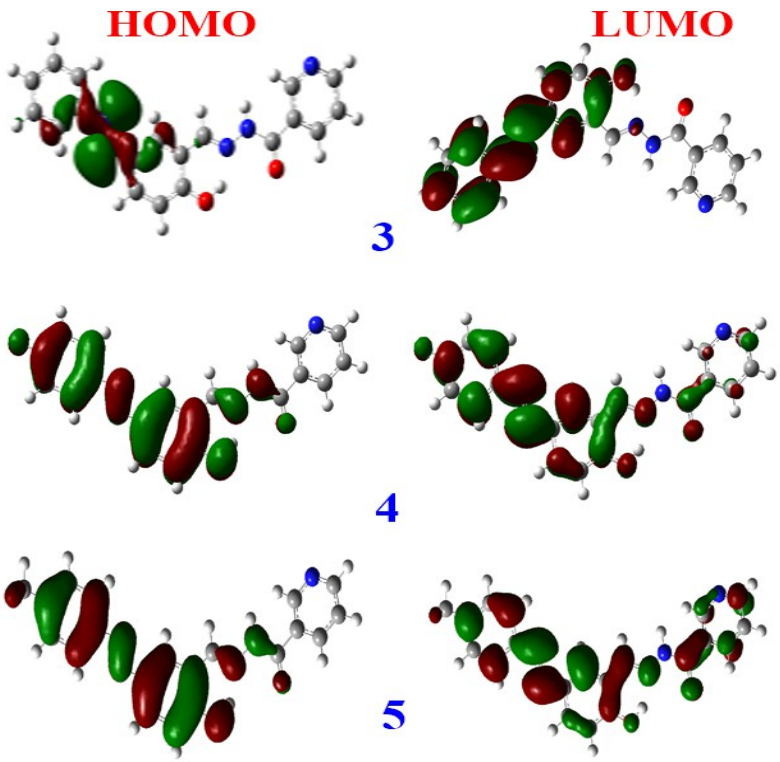

Fig. 2. HOMO-LUMO picture of 3-5

3.6. HOMO-LUMO energies, dipole moments

HOMO-LUMO energies and dipole moments for the hydrazides **3-5** were calculated and the values are listed in **Table 6**. HOMO-LUMO pictures are reproduced in **Fig. 2**. From **Table 6**, it is seen that the introduction of electron withdrawing fluoro at the *para* and *meta* of phenyl ring decreases the energies of both HOMO and LUMO orbitals whereas electron releasing methyl substituents increase the energies of both HOMO and LUMO orbitals. Introduction of substituents at the phenyl ring decreases the energy gap (ΔE).

The dipole moment is higher in hydrazide **5** whereas in other compounds the dipole moments are lower compared to the parent hydrazide **3**. The electronic chemical potential 'μ' which is a characteristic of electronegativity defined by Parr and Pearson[22] and hardness 'η' have been calculated using the formulae $\mu = -½ [E_{HOMO} + E_{LUMO}]$, $\eta = ½ [E_{LUMO} - E_{HOMO}]$ and the values are also listed in **Table 6**. The higher HOMO energy corresponds to the more reactive molecule in the reactions with electrophiles, while lower LUMO energy is essential for molecular reactions with nucleophiles.[23]

Table 6. HOMO-LUMO energies (eV), electronegativities, hardness and dipole moments μ(D) for 3-5

Compds.	HOMO-LUMO energies			Dipole moments				η	μ
	LUMO	HOMO	ΔE	μ_x	μ_y	μ_z	μ_{tot}		
3	-2.132	-5.745	3.613	0.675	-3.284	0.995	3.497	1.807	3.939
4	-2.184	-5.761	3.577	1.815	-2.819	0.968	3.489	1.789	3.973
5	-2.063	-5.647	3.584	-0.194	-3.548	0.997	3.690	1.792	3.855

3.7. NLO properties

The polarizabilities and first order polarizabilities were also calculated by finite field approach using the basis set B3LYP/6-31G* available in Gaussion-03 package and these values are listed in **Table 7**.

The calculated polarizability α_{ij} is dominated by the diagonal components (α_{xx}, α_{yy}, α_{zz}) and the hyperpolarizability β is dominated by the longitudinal components β_{xxx}, β_{xxy}, β_{xyy} and β_{xxz}. From this it is inferred that a substantial delocalization of charges is noticed in these directions. All the molecules are polar having non-zero dipole moment components and such compounds may have large microscopic hyperpolarizability and hence may have rather well microscopic NLO behaviour. The higher dipole moment values are associated in general with even larger projection of β_{tot} quantities.

In Table 7 the β_{tot} obtained for other hydrazides are also found to be greater than that of urea. The microscopic molecules with larger hyperpolarizability values will make macroscopic materials with strong non-linear optical properties. The observed β values indicate that the hydrazides **3-5** can be considered as better NLO materials than urea molecule.

The NLO character decreases according to the following order:

H (**3**) > *p*- CH_3 (**5**) > > *p*- F (**4**).

Table 7. The polarizability and hyperpolarizability of 3-5

	3	**4**	**5**
α_{xx}	547.321	556.757	587.783
α_{xy}	35.042	26.638	34.058
α_{yy}	284.955	282.389	293.625
α_{xz}	9.298	10.346	10.192
α_{yz}	5.786	6.072	6.003
α_{zz}	86.902	88.161	96.847
$<\alpha>$ (a.u)	306.393	309.102	326.085
$10^{24} \times \alpha_{tot}$ (esu)	45.407	45.809	48.326
β_{xxx}	–276.703	139.563	343.379
β_{xxy}	–1781.335	–1468.781	–1564.986
β_{xyy}	–370.712	–128.669	–103.180
β_{yyy}	9.783	60.935	59.690
β_{XXZ}	164.470	152.262	155.060
β_{xyz}	5.699	–4.632	–7.403
β_{yyz}	6.363	6.807	5.550
β_{xzz}	11.852	6.563	–26.007
β_{yzz}	2.407	–2.042	5.068
β_{zzz}	3.549	4.567	4.699
β_{tot} (a.u)	1887.905	1419.461	1524.431
$10^{33} \times \beta_{tot}$ (esu)	16310.179	12263.145	13170.014

4. CONCLUSIONS

Hydrazides **3–7** were synthesized and characterized by spectral studies. The dipole moment, polarizability and first order polarizability were also computed and calculated. NBO analysis shows that the transfer of electrons occurs from phenyl ring to azo linkage. The AIM reveals the presence of intramolecular hydrogen bond. The HOMO-LUMO and MEP indicate the reactivity of the molecule.

References

[1] D.A. Williams and T.L. Lemke (Eds.), Foye's Principles of Medicinal Chemistry, 5th edn., Lippincott Williams and Wilkins, Philadelphia, **2002**.

[2] L.M. Prescott, J.P. Harley and D.A. Klein (Eds.), In: Microbiology, 2nd edn., WMC Brown Publishers, Oxford, England, **1990**, p. 328.

[3] A. Madhukar, N. Kannappan, A. Deep, P. Kumar, M. Kumar and V. Prabhakar, Int. J. Chem. Tech. Res., **2009**, 1, 1376.

[4] K.K. Jha, A. Samad, Y. Kumar, M. Shaharyar, R.L. Khosa, J. Jain, V. Kumar and P. Singh, Eur. J. Med. Chem., **2010**, 45, 4963.

[5] M. Gallego, M. Garcia-Vargas and M. Valcarcel, Analyst, **1979**, 104, 613.

[6] M. Gallego, M. Garcia-Vargas, F. Pino and M. Valcarcel, Microchem. J., **1978**, 23, 353.

[7] B.N. Bessy Raj and M.R. Prathapachandra Kurup, Spectrochim. Acta A, **2007**, 66, 898.

[8] R. Benassi, A. Benedetti, F. Taddei, R. Cappelletti, D. Nardi and A. Tajana, Org. Magn. Reson., **2005**, 20, 26.

[9]. A. Manimekalai, B. Senthil Sivakumar and T. Maruthavanan, Indian J. Chem. B, **2004**, 43, 1753.

[10] N.M. Hosny, J. Mol. Struct., **2009**, 923, 98.

[11] P.N. Prasad, D.J. Williams, Nonlinear Optical Effects in Molecules and Polymers, Wiley, New York, **1991**.

[12] B.R. Thorat, P. Kamat, D. Khandekar, S. Lele, M. Mustapha, S. Sawant, R. Jadhav, S. Kolekar, R. Yamga and R.G. Atram, J. Chem. Pharm. Res., **2011**, 3,1109.

[13] A. Kriza, M.L. Dianu, N. Stanica, C. Draghici and M. Popoiu, Rev. Chim., **2009**, 60, 555.

[14] N.K. Singh and D.K. Singh, Synth. React. Inorg. Met. Org. Chem., **2002**, 32, 203.

[15] M. Odabasoglu, C. Albayrak, R. Ozkanca, F.Z. Aykan, P. Lonecke, J. Mol. Struct. **2007**, 840, 71-89.

[16] M.J. Frisch, G.W. Trucks, H.B. Schlegel, G.E. Scuseria, M.A. Robb, J.R. Cheeseman, V.G. Zakrzewski, J.A. Montgomery Jr., R.E. Stratmann, J.C. Burant, S. Dapprich, J.M. Millam, A.D. Daniels, K.N. Kudin, M.C. Strain, O. Farkas, J. Tomasa, V. Barone, M. Cossi, R. Cammi, B. Mennucci, C. Pomeli, C. Adamo, S. Clifford, J. Ochterski, G.A. Peterson, P.Y. Ayala, Q. Cui, K. Morokuma, P. Salvador, J.J. Dannenberg, D.K. Malick, A.D. Rabuck, K. Raghavachari, J.B. Poresman, J. Cioslowski, J.N. Ortiz, A.G. Babboul, B.B. Stefavov, G. Liu, A. Liashenko, P. Piskorz, I. Komaromi, R. Gomperts, R.L. Martin, D.J. Fox, T. Keeth, M.A. Allaham, C.Y. Peng, A. Nanayakkara, M.W. Wong, J.L. Anders, C. Gonzales, M. Challacombe, P.M. Gill, B. Johnson, W. Chen, M. Head-Gordon, E.S. Replogle, J.A. Peple, Gaussian 98, Revision A. 9, Pittsburg, Pa: Gaussian IC, 2001.

[17] R.M. Silverstein and F.X. Webster, Spectrometric Identification of Organic Compounds, 6th edn., John Wiley and Sons, New York, **1996**.

[18] W. Kemp, Organic Spectroscopy, The Macmillan Press Ltd., **1975**, 14, 1375.

[19] S. Miertus and J. Tomasi, Chem. Phys., **1982**, 65, 239.

[20] R.F.W. Bader, Atoms in Molecules: A Quantum Theory, Oxford University Press, Oxford, **1990**.

[21] T.A. Keith, AIM All (Version 11.04.03) (aim.tkgriskmill.com), 2011.

[22] R.G. Parr and R.G. Pearson, J. Am. Chem. Soc., **1983**, 105, 7512.

[23] A. Rauk, Orbital Interaction Theory of Organic Chemistry, 2nd edn., John Wiley and Sons, New York, **2001**, 34.